Available online at www.sciencedirect.com
SCIENCE DIRECT®
ELSEVIER
European Journal of Mechanics B/Fluids 23 (2004) 17–27
EUROPEAN JOURNAL OF MECHANICS B/FLUIDS

Critical mass in vortex-induced vibration of a cylinder

R. Govardhan [a,*], C.H.K. Williamson [b]

[a] *Mechanical Engineering, Indian Institute of Science, Bangalore-560012, India*
[b] *Mechanical and Aerospace Engineering, Upson Hall, Cornell University, Ithaca, NY 14853, USA*

Received 31 March 2003; accepted 30 April 2003

Abstract

In this paper, we study the transverse vortex-induced vibrations of a cylinder at low mass-damping values. The response in this case consists of three distinct branches; namely the initial, upper and lower branches. For an elastically-mounted cylinder, the oscillation frequency can be shown to be primarily dependent on the mass ratio (m^* = mass/displaced fluid mass). For large mass ratios, $m^* = \mathrm{O}(100)$, the vibration frequency for synchronization lies close to the natural frequency ($f^* = f/f_\mathrm{N} \sim 1.0$), but as mass is reduced to $m^* = \mathrm{O}(1)$, f^* can reach remarkably large values. We deduce an expression for the frequency of the lower-branch vibration, at small mass-damping values, as follows:

$$f^*_\mathrm{lower} = \sqrt{\frac{m^* + 1}{m^* - 0.54}}$$

which agrees very well with a wide set of experimental data. This frequency equation indicates the existence of a *critical mass ratio*, where the frequency f^* becomes large:

$$m^*_\mathrm{crit} = 0.54.$$

When $m^* < m^*_\mathrm{crit}$, it can be shown that the lower branch can never be reached and ceases to exist. In this case, the upper branch regime of synchronisation is predicted to continue to infinite normalized flow speed, $U^* \to \infty$, where $U^* = U/f_\mathrm{N} D$ is the conventionally used normalized flow speed.

In the case of a cylinder with no structural restoring force, the natural frequency f_N is zero, and therefore the conventionally defined U^* is infinite. Experiments under these conditions indicate that there are negligible oscillations as mass ratio is reduced from large values to m^* of the order of unity. However, a further reduction in mass exhibits a surprising result; large-amplitude oscillations suddenly appear for values of mass less than a critical mass ratio of 0.542. This result for the critical mass from experiments with a cylinder having no structural restoring force is in remarkable agreement with the earlier predictions from the elastically-mounted cylinder experiments.

Keywords: Vortex; Vibration; Critical mass; Cylinder; Dynamics

1. Introduction

Vortex-induced vibrations of cylinders have been studied extensively, as may be seen from the reviews of Sarpkaya [1], Bearman [2] and Parkinson [3]. In the present work, we study the effect of mass ratio (m^* = mass/displaced mass) on the response of such an oscillating cylinder. Both the conventional elastically-mounted cylinder and also a cylinder where the structural restoring force is zero, i.e., with the springs removed, are used in this study.

* Corresponding author.
E-mail addresses: raghu@mecheng.iisc.ernet.in (R. Govardhan), cw26@cornell.edu (C.H.K. Williamson).

0997-7546/$ – see front matter
doi:10.1016/j.euromechflu.2003.04.001

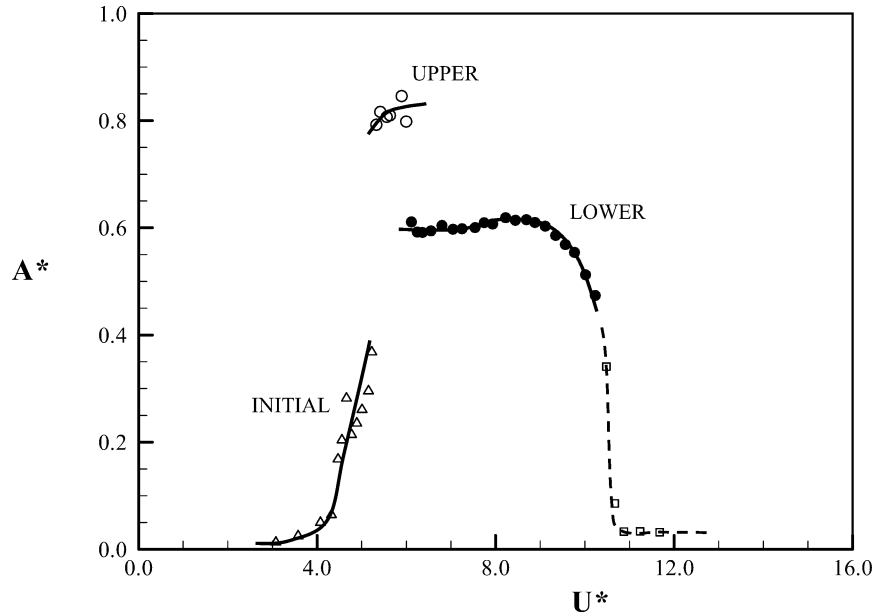

Fig. 1. *Low mass-damping case exhibiting 3-modes*. Amplitude response as a function of flow speed, showing three response branches; namely the Initial, Upper and Lower ($m^* = 8.63$, $(m^* + C_A)\zeta = 0.0185$). △, initial; ∘, upper; •, lower; □, desynchronized regime.

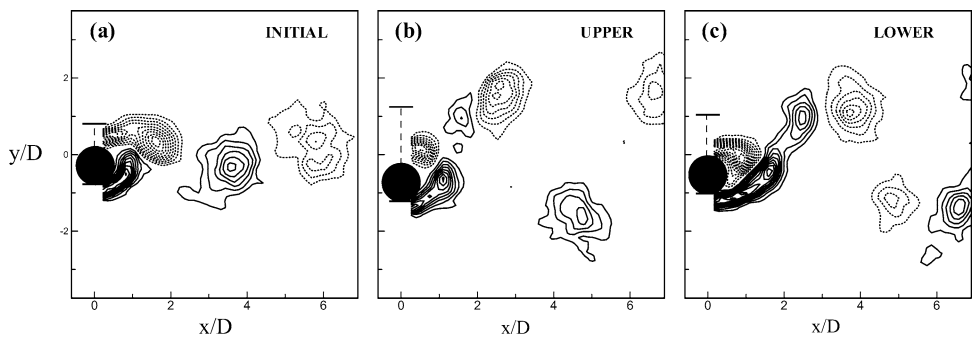

Fig. 2. Vortex formation modes in the different response branches. (a) Initial branch – 2S; (b) Upper branch – 2P; (c) Lower branch – 2P. In the Upper branch case, there are two vortex pairs formed per cycle, although the second vortex of each pair is much weaker than the first vortex, and decays rapidly. Vorticity contours levels shown are separated by $\Delta(\omega D/U) = 0.4$. Solid contour lines denote anticlockwise vorticity and dashed lines are for clockwise vorticity. 2S, 2P modes are as defined by Williamson and Roshko [7].

The response of an elastically-mounted cylinder free to vibrate transverse to the flow has been studied extensively since the early work of Feng [4]. For low values of mass-damping ($m^*\zeta$), recent studies by Khalak and Williamson [5] and Govardhan and Williamson [6] indicate that there exist three response branches; namely the initial, upper and lower, as shown in Fig. 1. (The mass ratio, $m^* =$ (oscillating mass)/(displaced fluid mass); and the damping ratio, $\zeta =$ structural damping/critical damping.) The relationship between the response, forces and wake dynamics for such an oscillating cylinder is studied in detail in Govardhan and Williamson [6].

Vorticity contours corresponding to the different response branches shown in Fig. 2, indicate that the Initial branch is associated with the 2S wake mode, while both the Upper and Lower branches correspond to the 2P-mode; '2S' indicating 2 Single vortices formed per cycle, and '2P' meaning 2 Pairs of vortices formed per cycle, as defined by Williamson and Roshko [7] based on their forced oscillation experiments. As may be seen from Fig. 2, the strengths of the two vortices of each vortex pair are quite unequal in the Upper branch, but are roughly equal in the Lower branch. In the case of forced vibration, the 2S and 2P modes have also been shown using PIV by Carberry, Sheridan and Rockwell [8] for the forced transverse vibration of a circular cylinder, and these modes are also observed from forced oscillations of a tapered cylinder by Techet et al. [9].

In the present paper, we shall study the effect of mass ratio on the response of a cylinder free to vibrate transverse to the flow at low values of mass-damping. We shall show using both the conventional case of an elastically-mounted cylinder and the limiting case of a cylinder with no structural restoring force that there exists a critical mass, which when crossed, leads to dramatic changes in the response.

2. Experimental details

The present experiments were conducted using a hydroelastic facility, which is described in Khalak and Williamson [5], in conjunction with the Cornell-ONR Water Channel. The hydroelastic facility comprises a carriage mounted on air-bearings situated above the channel test-section, which allows a vertical cylinder in the fluid to move transverse to the free-stream. As there is no metal-metal contact, the damping associated with the air-bearing system is extremely small, and therefore in all cases reported here the mass-damping parameter is also very small ($(m^* + C_A)\zeta < 0.05$). The turbulence level in the test section of the Water Channel was less than 0.9%, in the 0.381 m × 0.508 m cross section, over the range of free stream velocities U (0.04–0.32 m · s^{-1}) used in this study. Test cylinders of diameters 0.0381 m and 0.0794 m were used for the elastically-mounted case and the zero structural restoring force case, respectively. The corresponding length-diameter ratios were 10 and 6, respectively.

For the purpose of employing DPIV, the flow was seeded with 14-micron silver-coated glass spheres, which were illuminated by a sheet of laser light from a 5W Argon ion laser. Pairs of particle images were captured using a high-resolution CCD Kodak Megaplus (1008 × 1018 pixels) camera, and analyzed using cross-correlation of sub-images, our implementation of which is described in more detail in Govardhan and Williamson [6].

3. Critical mass: frequency response of an elastically-mounted cylinder

The oscillation frequency (f) of an elastically-mounted cylinder depends primarily on the mass ratio (m^*), as discussed for example in Bearman [2]. This may be seen clearly from the equation for the cylinder frequency response ($f^* = f/f_N$) shown below, which is formulated here along the lines of Khalak and Williamson [5], as follows:

$$f^* = \sqrt{\frac{m^* + C_A}{m^* + C_{EA}}}, \tag{1}$$

where C_{EA} is the effective added mass due to wake vortex dynamics, and C_A is the potential added mass ($C_A = 1.0$ for a circular cylinder).

At high mass ratios, the large m^* values overwhelm the effect of the effective added mass (C_{EA}), thus yielding $f^* = f/f_N \approx 1.0$. Hence, at high mass ratios, as in Feng [4], the response frequency (f) is close to the natural frequency (f_N) in the synchronization regime. On the other hand, at low m^* the effective added mass (C_{EA}) influences f^* significantly, and results in a marked deviation of f^* from unity. This has been seen for example in more recent experiments of Moe and Wu [10], Khalak and Williamson [11] and Govardhan and Williamson [6].

The effect of mass ratio on the amplitude response is illustrated by the two example cases shown in Fig. 3. As observed by Griffin and Ramberg [12], the amplitude response for the lower mass ratio case indicates a widening of the region of vigorous synchronized oscillations (in $U^* = U/f_N D$) compared to the larger m^* case. However, as shown by Khalak and Williamson [5], when the two amplitude responses are plotted versus the parameter $(U^*/f^*)S$, which is equivalent to (f_{vo}/f), then the data sets collapse very well especially in the lower branch, as shown in Fig. 4 (f_{vo} = non-oscillating body vortex shedding frequency; f = body oscillation frequency; S = Strouhal number).

A striking aspect of the frequency response is the almost constant value for the lower branch frequency over the complete response branch. This constant level of frequency is observed in both cases shown in Fig. 3 and at every mass ratio investigated ($m^* = 0.8$ to 20), and seems to be a general characteristic of this lower branch. This observation is also supported by the frequency data of Hover et al. [13] and Khalak and Williamson [5], both at similar low mass-damping values.

A large set of data for the Lower branch frequency (f^*_{lower}) plotted versus m^*, is shown in Fig. 5. This data is from our own experiments, and from the low mass-damping experiments of Hover et al. [13], Khalak and Williamson [5], and Anand [14]. The data collapse very well onto a single curve. Since the response in the lower branch is remarkably sinusoidal and periodic, Eq. (1) is a very good representation of the frequency response. The effective added mass (C_{EA}) in Eq. (1) is itself a function of $\{(f_{vo}/f), A^*\}$, and will have a unique value along the lower branch data, when plotted in the plane $\{(f_{vo}/f), A^*\}$ as in Fig. 4. Since at low values of mass-damping, $(m^* + C_A)\zeta < 0.05$, all lower-branch data sets lie nearly along the same line in this plane, almost independently of mass ratio, m^*, the value of C_{EA} along this line will be independent of m^*. Further, in the lower

branch, the frequency response, f^*, is nearly a constant for any given mass ratio, and Eq. (1) therefore indicates that C_{EA} is a constant along the entire collapsed lower branch data in Fig. 4. This implies that there is a single value of C_{EA} that represents all the lower branch frequency data, which may be found as the best fit of C_{EA} in Eq. (1) that represents the experimental data of Fig. 5. From this analysis, we find $C_{EA} = -0.54 \pm 0.02$, and we thereby deduce the following Lower-branch frequency equation as:

$$f^*_{\text{lower}} = \sqrt{\frac{m^* + 1.0}{m^* - 0.54}}. \tag{2}$$

This curve is drawn through the data in Fig. 5, and it represents the data very well.

An important consequence of Eq. (2) is that the frequency becomes infinite as the mass ratio reduces to the limiting value of 0.54. Therefore we conclude that there exists a critical mass ratio:

$$\text{Critical mass ratio,} \quad m^*_{\text{crit}} = 0.54. \tag{3}$$

The existence of a critical mass is, for us, a surprising and interesting result.

As the mass ratio decreases, the normalized velocity U^* for the start of the lower branch varies, maintaining the condition seen in Fig. 4:

$$(f_{\text{vo}}/f)_{\text{start}} = 1.15. \tag{4}$$

Since the frequency ratio (f_{vo}/f) may also be written in terms of the normalized flow speed, U^*, as $(f_{\text{vo}}/f) = (U^*/f^*)S$, we can rewrite the above condition in terms of U^* for the start of the lower branch (U^*_{start}) by using Eq. (2) and assuming $S = 0.2$ as:

$$U^*_{\text{start}} = 5.75\sqrt{\frac{m^* + 1.0}{m^* - 0.54}}. \tag{5}$$

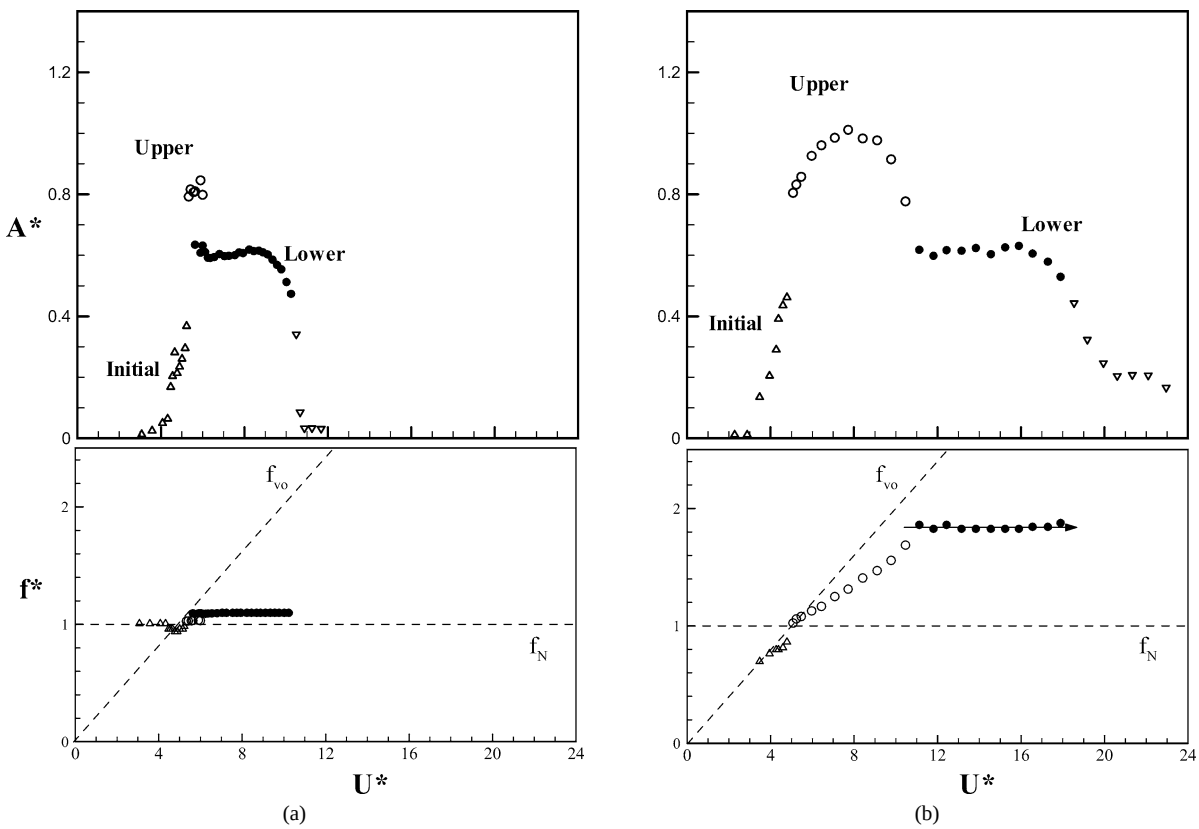

Fig. 3. Amplitude – frequency plots for (a) $m^* = 8.6$, and (b) $m^* = 1.2$, plotted to the same scale. The mass-damping parameter is small in both cases; (a) $(m^* + C_A)\zeta = 0.02$, (b) $(m^* + C_A)\zeta = 0.01$. f_{vo} is the stationary body vortex shedding frequency and f_N is the structural natural frequency. △, initial; ○, upper; ●, lower; ▽, desynchronized.

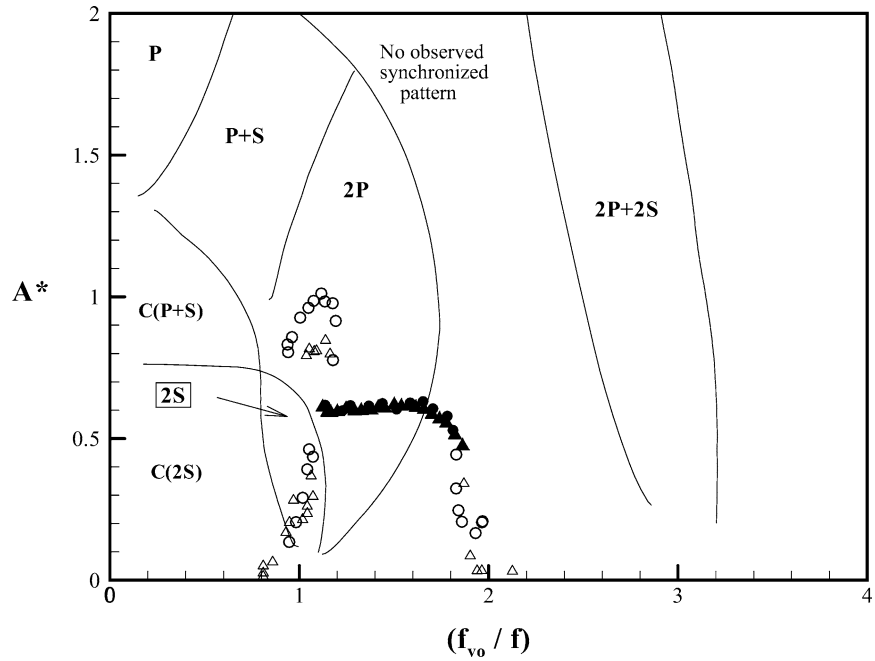

Fig. 4. Amplitude response for two different mass ratios (m^*) plotted versus the frequency ratio (f_{vo}/f), where f_{vo} is the stationary body vortex shedding frequency and f is the body oscillation frequency. ○, $m^* = 1.19$ and $(m^* + C_{\mathrm{A}})\zeta = 0.0110$; △, $m^* = 8.63$ and $(m^* + C_{\mathrm{A}})\zeta = 0.0185$. Solid symbols indicate the Lower branch regimes. —, Williamson and Roshko [7] map of wake modes.

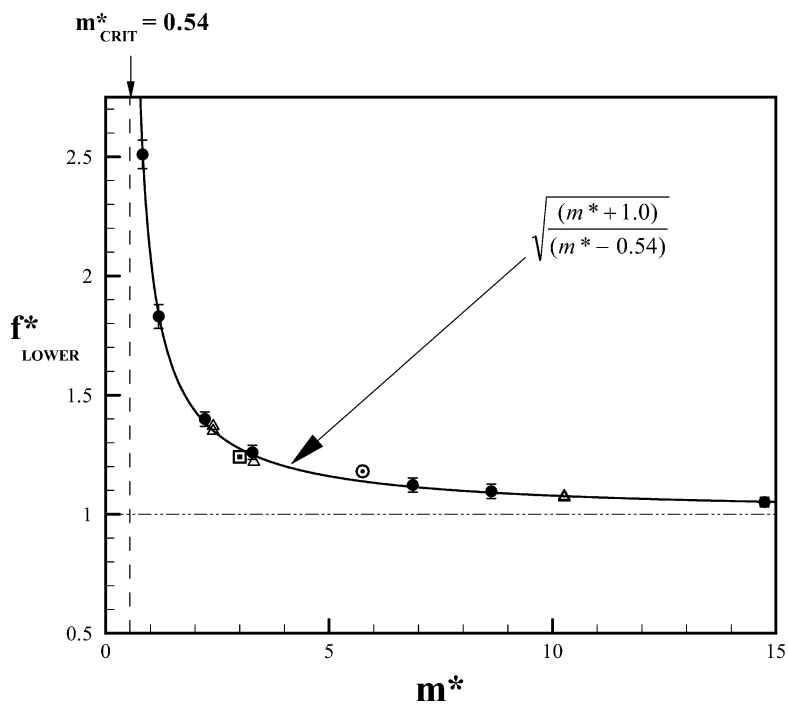

Fig. 5. Variation of the lower-branch frequency (f^*_{lower}) as a function of the mass ratio m^*. The equation for f^*_{LOWER} fits the data remarkably well, and indicates a dramatic increase in f^*_{LOWER} as we approach the critical mass ratio, $m^*_{\mathrm{CRIT}} = 0.54$. •, Present data; △, Khalak and Williamson [5]; ⊡, Hover et al. [13]; ⊙, Anand [14].

This shows that the velocity for the start of the Lower branch:

$$U^*_{\text{start}} \to \infty \quad \text{as } m^* \to m^*_{\text{crit}}.$$

Therefore, when mass ratios fall below $m^*_{\text{crit}} = 0.54$, the Lower branch cannot be reached and ceases to exist. We conclude that the Upper branch will continue indefinitely, and the synchronization regime will extend to infinity!

4. Critical mass: cylinder with zero structural restoring force

The prediction of large-amplitude response at infinite U^* suggested by the elastically-mounted cylinder experiments in the previous section, may be directly verified by experiments with a cylinder having zero structural restoring force, i.e., a cylinder with no springs attached. In this case, the natural frequency, f_{N}, is zero, and therefore the conventional normalized velocity, $U^* = U/f_{\text{N}}D = \infty$.

The response time trace for a very low mass ratio, $m^* = 1.67$, cylinder is shown in Fig. 6(a) and does indeed seem intriguing. Despite the fact that one could move the cylinder, mounted on air-bearings, simply by brushing it with a feather, we found that the body remained stationary. This was surprising to us given that the cylinder is completely free to move transverse to the flow, and is subjected to large transverse (lift) forces, as may be inferred from the strong periodic shedding of vortices shown in Fig. 7(a). However, simply by reducing the mass ratio to $m^* = 0.45$, we discovered large-amplitude oscillations to occur. These vigorous oscillations (in Fig. 6(b)) were at amplitudes of the order of $A^* = A/D \approx 0.80$. The wake vortex dynamics for this case shown in Fig. 7(b) was observed to be an unequal '2P' wake mode; the pattern being reminiscent of the wake vortex pattern found in the 'upper' branch of response for an elastically-mounted cylinder shown in Fig. 2.

It should be noted that the oscillation amplitudes and also the normalized oscillation frequency (f/f_{vo}) remained nearly independent of flow speed over a wide range of flow velocities (or Reynolds numbers) investigated, at a fixed mass ratio, as

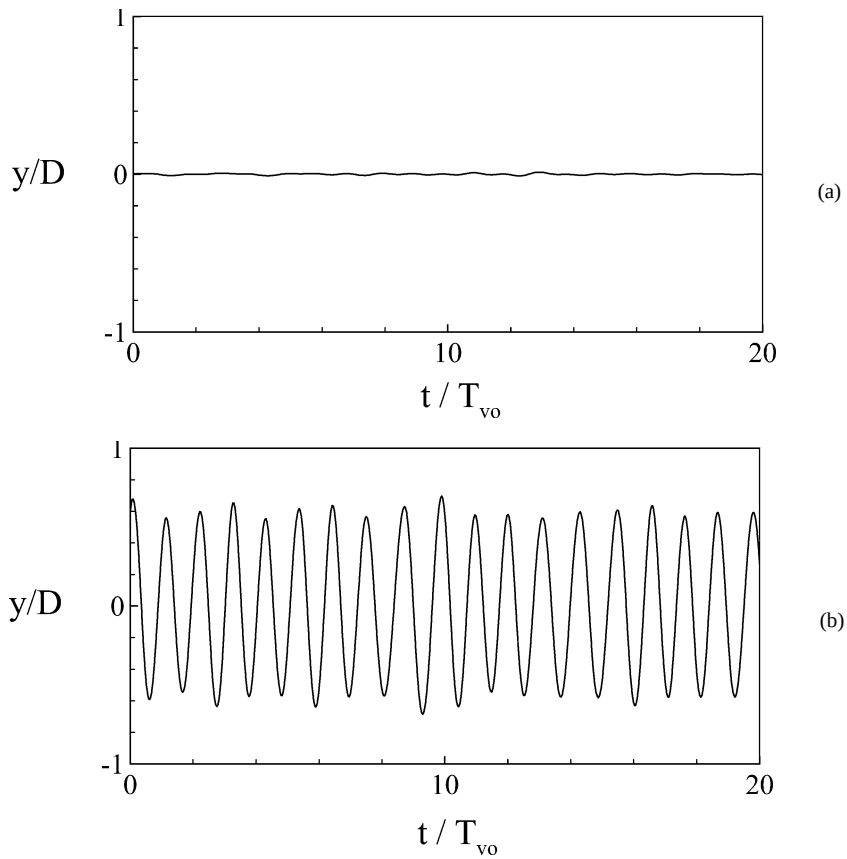

Fig. 6. Time trace of response for a cylinder with no springs for (a) $m^* = 1.67$, and (b) $m^* = 0.45$. In (a), no significant oscillations are observed, while in (b) large-amplitude oscillations are seen. $Re \approx 5100$ in both cases.

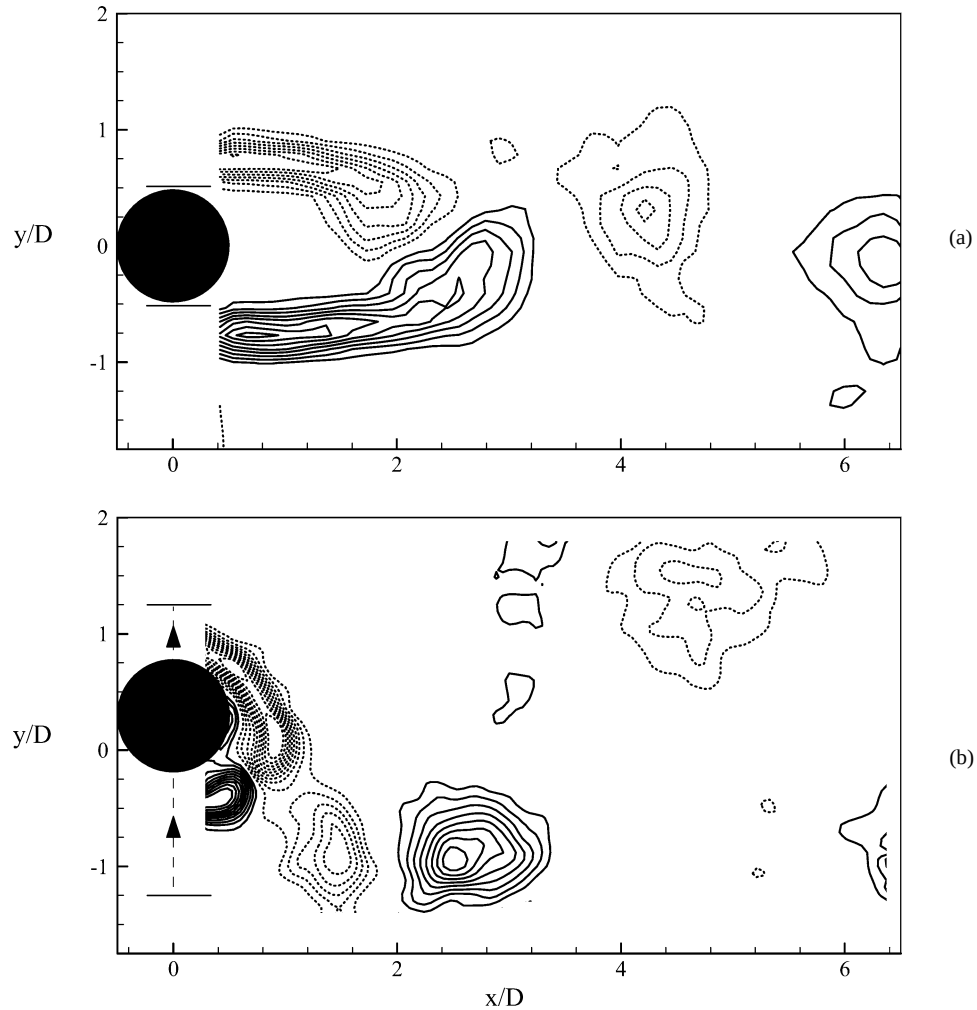

Fig. 7. Vorticity plots from DPIV, for a cylinder vibrating without springs, showing in (a), the 2S wake mode for the nearly non-oscillating case ($m^* = 1.67$), and in (b), the 2P mode for a lower mass ratio case ($m^* = 0.45$) that exhibits large-amplitude oscillations. In (b), two vortex pairs are formed per cycle, although the second vortex of each pair is weaker than the first, and decays rapidly. Vorticity contour levels shown are separated by $\Delta\omega D/U = 0.5$. Solid contour lines denote anticlockwise vorticity and dashed lines are for clockwise vorticity. $Re \approx 5100$ in both cases.

may be seen from Fig. 8. There is therefore a collapse of the response data (over all the flow speeds) to a single point on the $\{(f_{\mathrm{vo}}/f), A^*\}$ plane, as shown in Fig. 9. We refer to this point as the 'Operating Point' in accordance with Govardhan and Williamson [15]. The location of this operating point can be shown to be primarily a function of the mass ratio, at small values of mass-damping, as discussed in detail in Govardhan and Williamson [15].

The huge change in the dynamics of the cylinder, from essentially no oscillations to large-amplitude vibrations, triggered by only a small change in mass ratio from $m^* = 1.67$ to $m^* = 0.45$, suggests that there does indeed exist a critical mass ratio at which there is a sudden 'catastrophic' change in the body dynamics. Keeping this in mind, the mass ratio was decreased in small steps from the larger m^* value, and the result is shown in Fig. 10. It is clear that the cylinder suddenly starts to undergo large-amplitude vigorous oscillations as the mass ratio crosses a critical mass ratio:

$$\text{Critical mass ratio,} \quad m^*_{\mathrm{crit}} = 0.542 \pm 0.01. \tag{6}$$

For $m^* > m^*_{\mathrm{crit}}$, the cylinder is almost stationary, while for $m^* < m^*_{\mathrm{crit}}$, the cylinder exhibits large-amplitude oscillations.

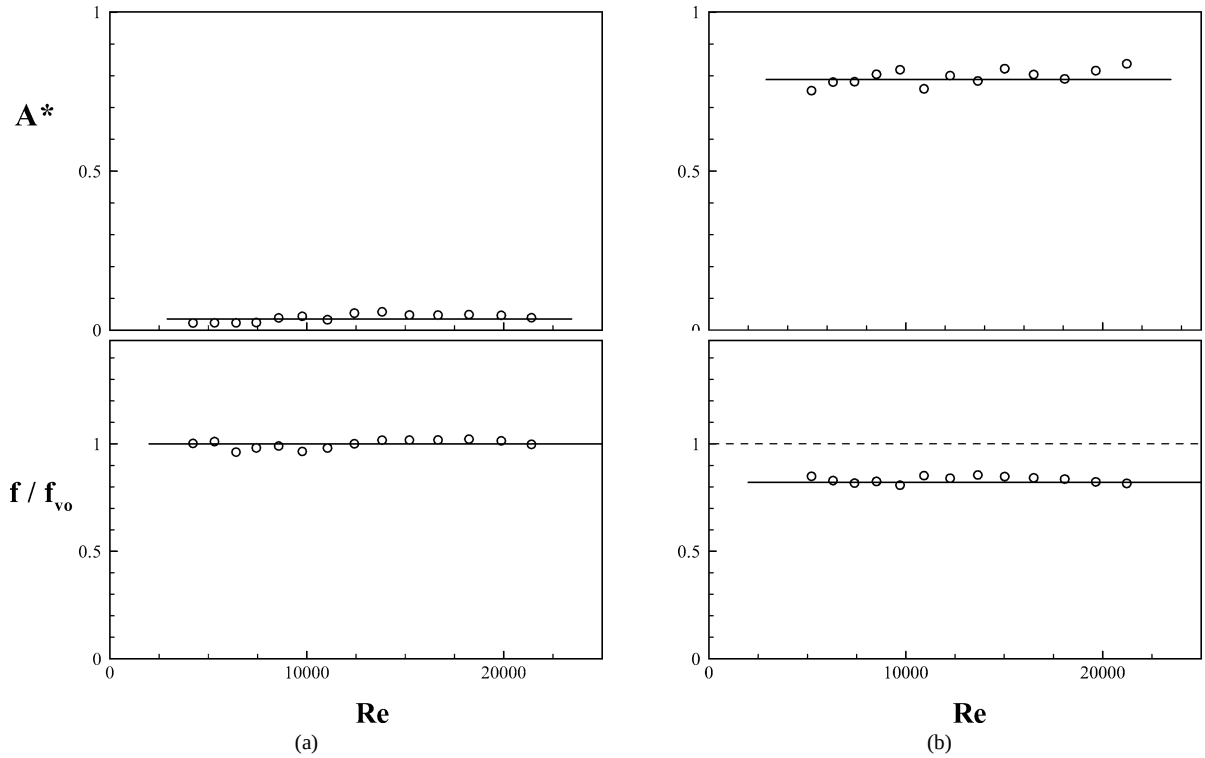

Fig. 8. Normalized response amplitude ($A^* = A/D$) and frequency ratio (f/f_{vo}) for a cylinder with no springs, showing that they remain at nearly the same value as the flow speed is varied. The mass ratios for the two cases are (a) $m^* = 1.67$, and (b) $m^* = 0.45$.

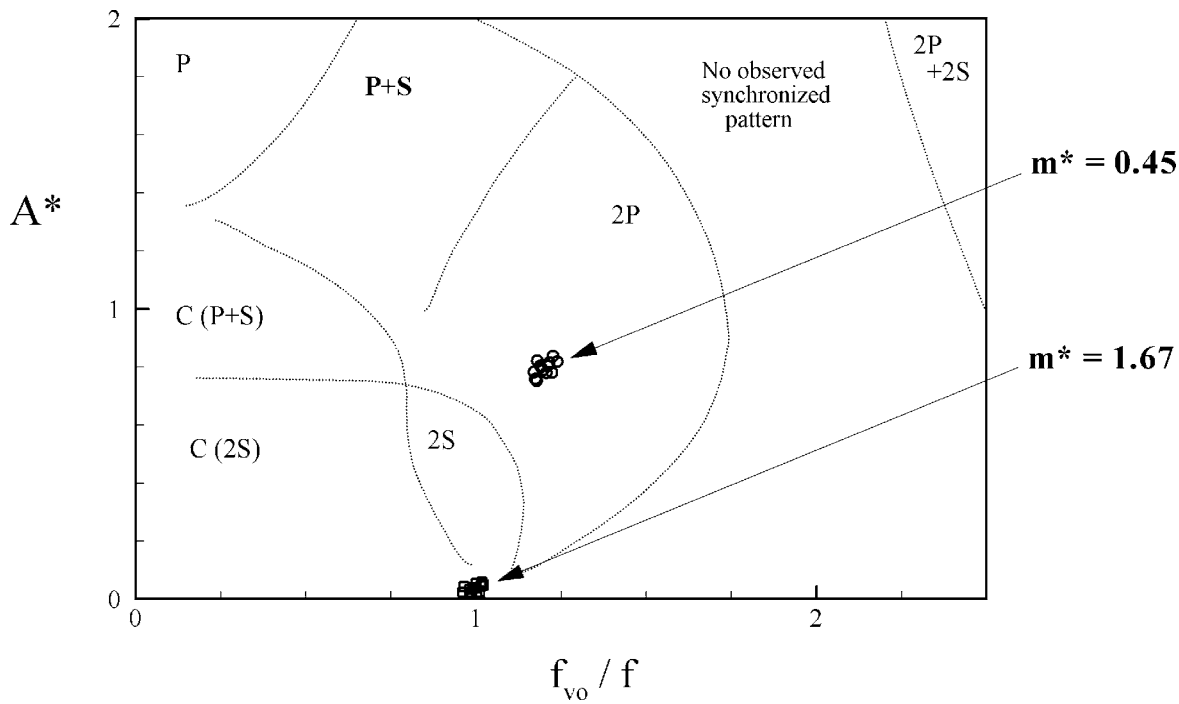

Fig. 9. Response data of Fig. 8 on the frequency-amplitude plane $\{(f_{vo}/f), A^*\}$, indicating that the oscillations are essentially independent of flow speed, in this plane. f_{vo} is the vortex shedding frequency in the absence of body oscillations, and f is the actual cylinder oscillation frequency. □, $m^* = 1.67$; ∘, $m^* = 0.45$; . . . , Williamson and Roshko [7] map of wake modes.

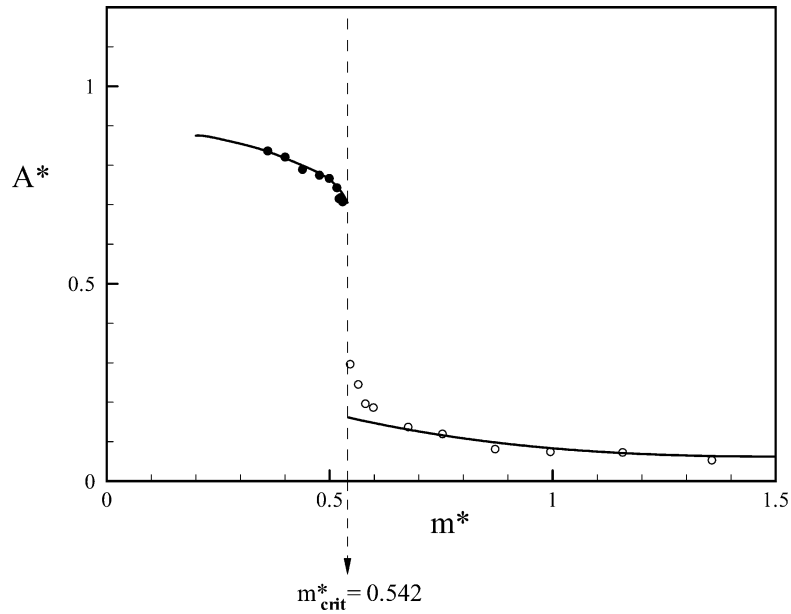

Fig. 10. Existence of a critical mass for a cylinder with no springs. Amplitude response (A^*) as mass ratio (m^*) is decreased, showing the sudden appearance of large-amplitude oscillations for m^* less than a critical value (m^*_{crit}) of 0.542. •, $m^* < m^*_{crit}$; o, $m^* > m^*_{crit}$.

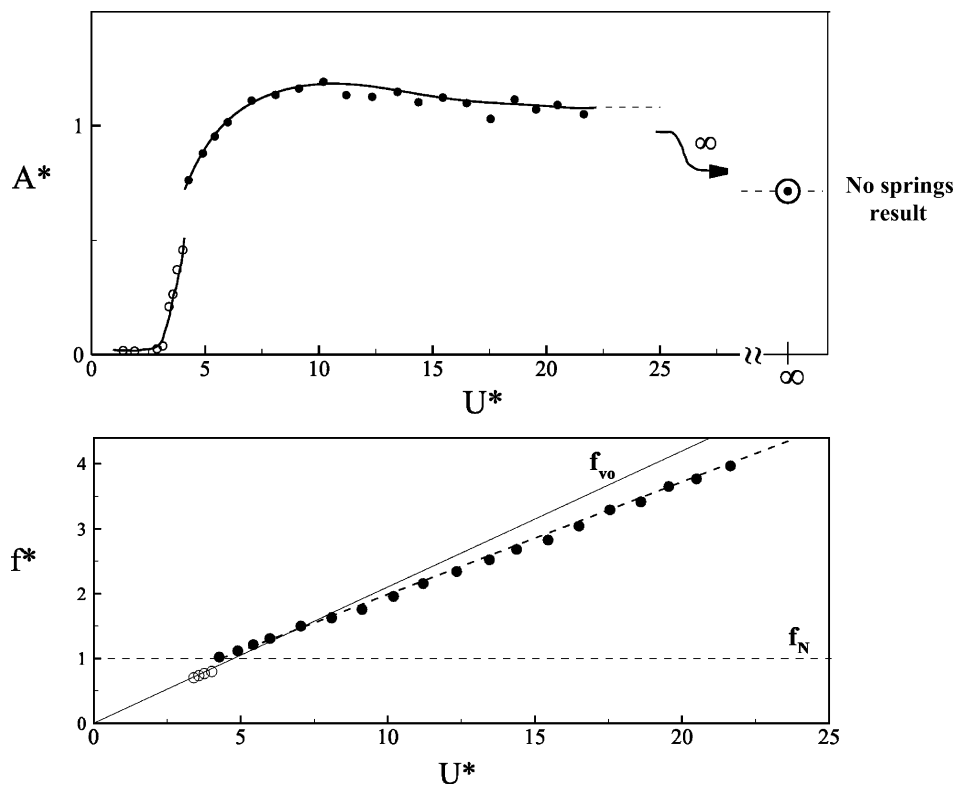

Fig. 11. Response for $m^* < m^*_{crit}$, showing an infinite regime of 'resonance'. The response amplitude at $U^* = \infty$, which corresponds to experiments without springs, remains large ($A^* \approx 0.7$). In this case, $m^* = 0.52$. o is for the initial branch; • is for the upper branch; ⊙ is for the experiments with no springs ($U^* = \infty$).

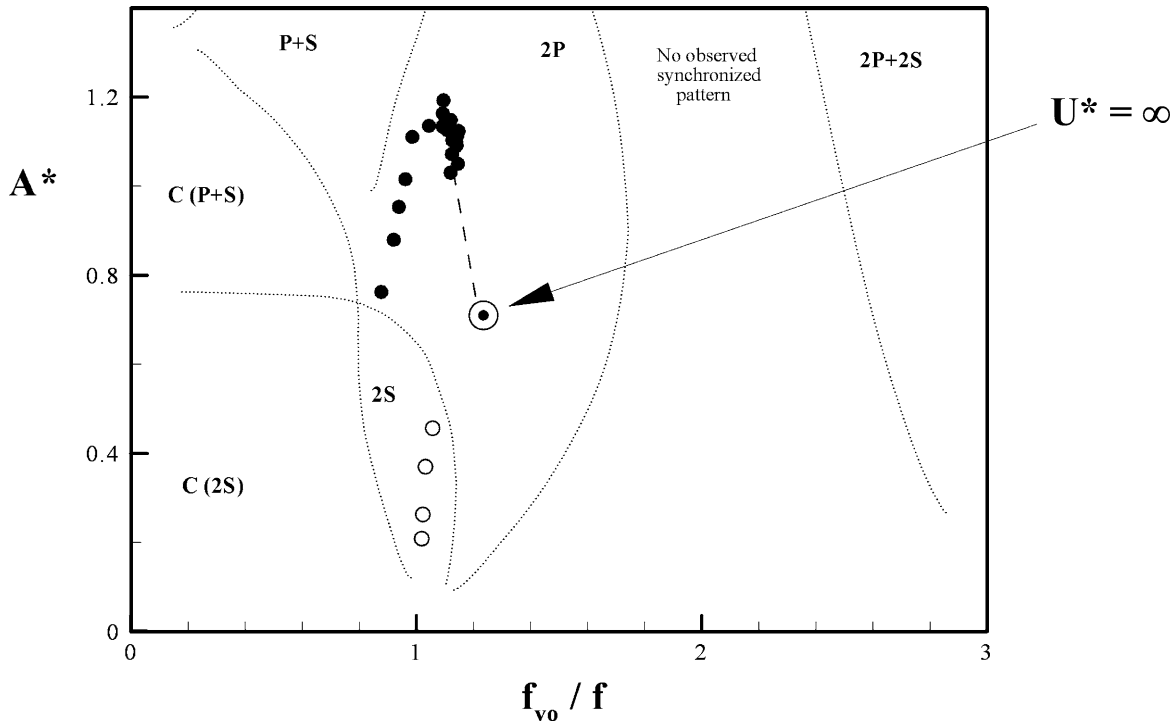

Fig. 12. Response data for $m^* < m^*_{\text{crit}}$ on the $\{(f_{\text{vo}}/f), A^*\}$ plane showing that the response gradually approaches a fixed 'operating point' as U^* is increased to infinity. Data shown here is identical to that in Fig. 11.

5. Critical mass and infinite regime of synchronization

The critical mass results from the cylinder with no structural restoring force case, is in remarkable agreement, both conceptually and numerically, with the predictions from the elastically-mounted cylinder experiments of Section 3. There are indeed large amplitude oscillations even at infinite U^*, when $m^* < m^*_{\text{crit}} = 0.54$. This implies that when $m^* < m^*_{\text{crit}}$, there will exist an infinitely wide range of flow speeds where vigorous oscillations occur, or in other words the regime of synchronization is infinitely wide. This result is distinctly different from the classical case, where significant oscillations occur only over a narrow range of flow speeds where the vortex shedding frequency, f_{V}, is of the order of the mechanical natural frequency, f_{N}, i.e., $f_{\text{V}} \sim f_{\text{N}}$.

The infinite regime of synchronization is illustrated in Fig. 11 for $m^* = 0.52$, and includes data both from elastically-mounted cylinder studies and also from cylinders with no springs corresponding to $U^* = \infty$. As may be seen the amplitude remains large at $U^* = \infty$, while the frequency continuously increases with U^*. Fig. 12 shows the same data as in Fig. 11, plotted in the plane of $\{(f_{\text{vo}}/f), A^*\}$, as done for the elastically-mounted case in Fig. 4. The data here gradually approach the "no springs" operating point, as the normalized flow speed U^* is increased.

6. Conclusions

In this paper, we study the transverse vortex-induced vibrations of a cylinder at low mass-damping values. The response in this case consists of three distinct branches; namely the initial, upper and lower branches.

In the elastically-mounted cylinder case, the oscillation frequency can be shown to be primarily dependent on the mass ratio ($m^* =$ mass/displaced fluid mass). For large mass ratios, $m^* = \text{O}(100)$, one expects from classical work that the vibration frequency will lie close to the natural frequency ($f^* = f/f_{\text{N}} \sim 1.0$). However, for very low mass ratios, $m^* = \text{O}(1)$, f^* can reach remarkably large values. We deduce an expression for the frequency of the lower-branch vibration, at small values of the mass-damping parameter, $(m^* + C_{\text{A}})\zeta < 0.05$, as follows:

$$f^*_{\text{lower}} = \sqrt{\frac{m^* + 1}{m^* - 0.54}}$$

which agrees very well with a wide set of experimental data. This frequency equation indicates the existence of a *critical mass ratio*, where the frequency f^* becomes large:

$$\text{Critical mass ratio,} \quad m^*_{\text{crit}} = 0.54 \quad \text{(elastically-mounted cylinder)}.$$

Also, we deduce an equation for the start of the lower branch:

$$U^*_{\text{start}} = 5.75\sqrt{\frac{m^* + 1.0}{m^* - 0.54}}$$

which indicates that when $m^* < m^*_{\text{crit}}$, the lower branch can never be reached and ceases to exist. In this case, the prediction is that the upper branch regime of synchronization continues to infinite normalized flow speed.

In the case of a cylinder with no structural restoring force, i.e., no attached springs, the natural frequency, f_{N}, is zero, and therefore the conventionally defined U^* is infinite. Experiments under these conditions with very low mass-damping values, indicate that there are negligible oscillations as mass ratio is reduced from large values to m^* of the order of unity. However, a further reduction in mass exhibits a surprising result; large-amplitude oscillations suddenly appear for values of mass less than a critical mass ratio of 0.542:

$$\text{Critical mass ratio,} \quad m^*_{\text{crit}} = 0.542 \quad \text{(cylinder with no springs)}.$$

This result for the critical mass from experiments with a cylinder having no structural restoring force is in remarkable agreement with the earlier predictions from the elastically-mounted cylinder experiments.

Acknowledgements

The support from the Ocean Engineering Division of O.N.R., monitored by Dr. Tom Swean, is gratefully acknowledged (O.N.R. Contract No. N00014-95-1-0332).

References

[1] T. Sarpkaya, Vortex-induced oscillations, ASME J. Appl. Mech. 46 (1979) 241–258.
[2] P.W. Bearman, Vortex shedding from oscillating bluff bodies, Annu. Rev. Fluid Mech. 16 (1984) 195–222.
[3] G. Parkinson, Phenomena and modelling of flow-induced vibrations of bluff bodies, Prog. Aerospace Sci. 26 (1989) 169–224.
[4] C.C. Feng, The measurements of vortex-induced effects in flow past a stationary and oscillating circular and D-section cylinders, Master's thesis, University of British Columbia, Vancouver, BC, Canada, 1968.
[5] A. Khalak, C.H.K. Williamson, Motions, forces and mode transitions in vortex-induced vibrations at low mass-damping, J. Fluids Structures 13 (1999) 813–851.
[6] R. Govardhan, C.H.K. Williamson, Modes of vortex formation and frequency response of a freely vibrating cylinder, J. Fluid Mech. 420 (2000) 85–130.
[7] C.H.K. Williamson, A. Roshko, Vortex formation in the wake of an oscillating cylinder, J. Fluids Structures 2 (1988) 355–381.
[8] J. Carberry, J. Sheridan, D. Rockwell, Forces and wake modes of an oscillating cylinder, J. Fluids Structures 15 (2001) 523–532.
[9] A.H. Techet, F.S. Hover, M.S. Triantafyllou, Vortical patterns behind a tapered cylinder oscillating transversely to a uniform flow, J. Fluid Mech. 363 (1998) 79–96.
[10] G. Moe, Z.-J. Wu, The lift force on a cylinder vibrating in a current, ASME J. Offshore Mech. Arctic Engrg. 112 (1990) 297–303.
[11] A. Khalak, C.H.K. Williamson, Fluid forces and dynamics of a hydroelastic structure with very low mass and damping, J. Fluids Structures 11 (1997) 973–982.
[12] O.M. Griffin, S.E. Ramberg, Some recent studies of vortex shedding with application to marine tubulars and risers, ASME J. Energy Resources Technol. 104 (1982) 2–13.
[13] F.S. Hover, A.H. Techet, M.S. Triantafyllou, Forces on oscillating uniform and tapered cylinders in crossflow, J. Fluid Mech. 363 (1998) 97–114.
[14] N.M. Anand, Free span vibrations of submarine pipelines in steady and wave flows, Ph.D. thesis, Norwegian Institute of Technology, Trondheim, Norway, 1985.
[15] R. Govardhan, C.H.K. Williamson, Resonance forever: existence of a critical mass and an infinite regime of synchronization in vortex-induced vibration, J. Fluid Mech. 473 (2002) 147–166.